Decreased Clock Gene Bmal1 Mediates Epileptogenesis via PCDH19 in Temporal Lobe Epilepsy

Hao Wu
The First Affiliated Hospital of Xi'an Jiaotong University
Yong Liu
The First Affiliated Hospital of Xi'an Jiaotong University
Lishuo Liu
The First Affiliated Hospital of Xi'an Jiaotong University
Qiang Meng
Department of Neurosurgery, The First Affiliated Hospital of Xi'an Jiaotong University
Changwang Du
The First Affiliated Hospital of Xi'an Jiaotong University
Kuo Li
The First Affiliated Hospital of Xi'an Jiaotong University
Shan Dong
The First Affiliated Hospital of Xi'an Jiaotong University
Yong Zhang
The First Affiliated Hospital of Xi'an Jiaotong University
Huanfa Li
The First Affiliated Hospital of Xi'an Jiaotong University
Hua Zhang (zhanghua@xjtu.edu.cn)
The First Affiliated Hospital of Xi'an Jiaotong University

Research

Keywords: Clock genes, Bmal1, Protocadherin 19, Dentate gyrus, Temporal lobe epilepsy, Transgenic mice

Posted Date: December 28th, 2020

DOI: https://doi.org/10.21203/rs.3.rs-133644/v1

Version of Record: A version of this preprint was published at Molecular Brain on July 14th, 2021. See the published version at https://doi.org/10.1186/s13041-021-00824-4.

Abstract

Clock genes not only regulate the circadian rhythm of physiological activities but also participate in the pathogenesis of many diseases. Previous studies have found the abnormal expression of clock genes in epilepsy. However, as the core clock gene, the molecular mechanism of Bmal1 in the epileptogenesis and seizures of temporal lobe epilepsy (TLE) is still unclear. To define the function of Bmal1, we firstly investigated the levels of Bmal1 and other clock proteins in the hippocampus in epilepsy. In the latency and chronic phases, the levels of Bmal1 were decreased compared with the control group. Knockout of Bmal1 in hippocampal dentate gyrus (DG) neurons of $Bmal1^{flox/flox}$ mice by Synapsin 1 (Syn1) promoter AAV (adeno-associated virus) lowered the threshold of seizures induced by pilocarpine administration. High throughput sequencing analysis showed that PCDH19 (protocadherin 19), a gene associated with epilepsy, was regulated by Bmal1. And the expression of PCDH19 was also decreased in the hippocampus of epileptic mice. Furthermore, the levels of Bmal1 and PCDH19 were higher in the patients with no hippocampal sclerosis (no HS), compared to HS International League Against Epilepsy (ILAE) type I and III. Altogether, these data suggest that decreased expression of clock gene Bmal1 may participate in the epileptogenesis and seizures via PCDH19 in TLE.

1. Introduction

Temporal lobe epilepsy (TLE) is one of the common drug-resistant epilepsy. The common pathological change of TLE is hippocampal sclerosis (HS) which is characterized by severe neuronal loss and gliosis in one or more hippocampal regions [1]. Patients with TLE are often accompanied by cognitive impairment, memory loss, and mood impairments. Despite a lot of effort, the pathogenesis of TLE remains incompletely unclear [2–4]. Clinical observation finds that patients with TLE show a 24-hour non-uniform distribution of seizure occurrence, and the number of seizures had unimodal (afternoon) or bimodal (morning and noon) time peaks [5–7]. Spontaneous seizures in kainic acid/pilocarpine-induced and electrically stimulated models of TLE have been found to occur in a pattern of 24-hour non-uniform distribution [8, 9]. These suggest that the epileptogenesis and seizures of TLE may be associated with the circadian rhythms.

Circadian rhythms are biological rhythms driven by a series of clock genes, such as Bmal1 (Brain and Muscle Arnt-Like Protein 1) and CLOCK (circadian locomotor output cycles kaput) [10]. As the core clock genes, Bmal1 and CLOCK in the cytoplasm heterodimerize and translocate to the nucleus, and then instigate transcription of target genes by interacting with E-box promoters. Among these target genes, some clock genes, such as Period (Per1/2/3) and Cryptochrome (Cry1/2), are involved in the positive and negative regulation of the circadian oscillation of Bmal1 and CLOCK. Clock genes and Clock-controlled genes (CCGs) underlie the rhythmic oscillations at a cellular and organismal level [11]. In the epileptic hippocampus, the levels of Bmal1, CLOCK, Cry and Per mRNA have been confirmed to be decreased. Previous studies have shown that the expression levels of clock genes change after seizures, and can regulate downstream genes to directly affect epileptogenesis [12, 13].

Several studies have investigated the role of Bmal1 in pathophysiology [14]. In the pilocarpine-induced epileptic rats, the level of Bmal1 mRNA is decreased in all comparison to the naive group [15]. The threshold of seizures induced by electrical stimulation in Bmal1 knockout (KO) mice is lower compared with the control group [16]. It should be pointed out that, in Ferraro's study, the ablation of Bmal1 is not specific in the specific brain nuclei and cellular types. Subsequent studies found that the ablation of Bmal1 in GLAST-positive astrocytes of the suprachiasmatic nucleus (SCN) alters circadian locomotor behavior and cognition in mice through GABA signaling [17]. Moreover, the Bmal1 deletion of astrocytes induces astrocyte activation and inflammatory gene expression via a cell-autonomous mechanism [18]. These studies suggest that abnormal expression of Bmal1 may be related to the epileptogenesis of TLE. However, it remains unclear how the changes of Bmal1 expression in the hippocampus, especially in hippocampal neurons, affect the epileptogenesis and seizures of TLE.

Therefore, in this study, we investigated the expression and distribution of Bmal1 in the hippocampus of TLE and tested the effects of Bmal1 conditional KO (cKO) in hippocampal neurons of Bmal1$^{flox/flox}$ mice on epileptogenesis and seizures. And the downstream genes regulated by Bmal1 were identified through high-throughput sequencing. Moreover, Bmal1 and downstream gene (PCDH19) were detected in the hippocampal specimens of patients with TLE.

2. Materials And Methods

2.1. Patient selection

The patients included in the study were obtained from the files of the Department of Neurosurgery, The First Affiliated Hospital of Xi'an Jiaotong University. We examined 16 specimens obtained from patients undergoing surgery for medically intractable TLE. All procedures were performed with the informed consent of the patients or legal next-of-kin and were approved by the Committee on Human Research at The First Affiliated Hospital of Xi'an Jiaotong University. Epilepsy was diagnosed according to the 2017 International Classification of Epileptic Seizures by the International League Against Epilepsy. Antiepileptic drug (AED) therapy had failed in all patients with maximum doses of at least three AEDs, including valproic acid, carbamazepine, phenytoin sodium, phenobarbital, clonazepam, topiramate, gabapentin, lamotrigine, and oxcarbazepine. Before surgery, patients were evaluated by multiple methods, including high-resolution magnetic resonance imaging (MRI), positron emission tomography (PET), long-term video electroencephalogram (EEG), and/or intraoperative electrocorticography (ECoG). Some of the patients underwent chronic intracranial EEG monitoring. Two neuropathologists reviewed all of the specimens independently. Supplementary table 1 summarizes the patients' clinical features.

2.2. Animals

Adult C57/BL6J mice weighing 20–25 g were purchased from the experimental animal center of Medical College in Xi'an Jiaotong University. Bmal1$^{flox/flox}$ mice were purchased from The Jackson Laboratory (Stock No: 007668). The animals were housed under controlled humidity (55 ± 5%) and temperature (20 ±

2 °C) with a normal 12 h light/12 h dark cycle. Water and food were available ad libitum. All animal procedures were carried out in line with the National Institutes of Health Guide for the Care and Use of Laboratory Animals and were ratified by the Institutional Animals Care and Use Committee. All procedures performed in studies involving animals were approved by the Ethics Committee of Xi'an Jiaotong University (Ethics and Science # G-83) in full accordance with the ethical guidelines of the National Institutes of Health for the care and use of laboratory animals. All efforts were made to minimize suffering and the number of rats used for the experiments.

2.3. Study design and experimental endpoints

To investigate the levels of proteins after seizures, 3 of 20 mice were randomly taken out and given saline vehicle as a control group, and the rest were administrated by pilocarpine to induce seizures. According to the Racine categories, 14 mice had seizures that reached Racine category 4 and were included in the epilepsy model group. Subsequently, 3 mice were randomly taken out at different time points (1d, 3d, 14d, 60d). Each mouse brain was divided into two parts along the longitudinal fissure. One part was used for immunoblotting experiments. The other part was fixed with 4% paraformaldehyde solution in PBS and used for immunofluorescence experiments. For evaluating the effects of Bmal1 conditional KO (cKO) on the susceptibility to seizures, 26 Bmal1$^{flox/flox}$ mice were randomly divided into 2 groups and injected Syn1-mCherry and Syn1-Cre AAVs respectively. Four weeks after AAVs injection, 3 mice were randomly selected from each group of animals to test the efficiency of Bmal1 cKO and transcriptome sequencing. Behavioral tests of 20 mice from the two groups are evaluated according to Racine categories. After behavioral tests, mice were sacrificed and collected samples for immunoblotting and immunofluorescence experiments.

2.4. Pilocarpine treatment and seizure assessment

Mice were administered intraperitoneally with methylscopolamine (1 mg/kg body weight) 30 min before injection of pilocarpine (300 mg/kg body weight) in 0.2 ml sterile saline vehicle (0.9% NaCl). Control mice received an equivalent volume of saline vehicle. The severity of seizure behavior was observed for 1 h and assessed using the following standard. Categories 1–2, one or more of the symptoms including facial automatisms, tail stiffening, and wet-dog shakes; Categories 1–2 were considered as a group to avoid subjectivity in assessing the seizures. Category 3 clonic unilateral forelimb myoclonus in addition to the symptoms above; Category 4 bilateral forelimb myoclonus and rearing; Category 5 generalized clonic-tonic convulsions and loss of postural control. The seizure categories were separately evaluated by two observers. A mouse experiencing continuous category 3–5 seizure events (30–90 sec) was considered to undergone status epilepticus (SE). Diazepam (10 mg/kg, i.p.) was administered to terminate SE 1 h after the onset. Mice were monitored for 2 h/day, 7 days/week for the occurrence of spontaneous seizures (category 3–5). Only after the occurrence of a seizure was a mouse identified as epilepsy mice (i.e. the observer was not aware of a priori of the treatment for any mouse). Methylscopolamine (S1978) and pilocarpine (S4231) were purchased from Selleck. Diazepam was purchased from Shanghai Shyndec Pharmaceutical Co., Ltd.

2.5. Total protein preparation and Immunoblotting

All mice were sacrificed under deep anesthesia with isofluorane (VETEASY, RWD Life Science). Then open the skull and carefully remove the brain tissue. Put the brain tissue in pre-cooled PBS, and separate the hippocampus from brain tissue with fine tweezers. Hippocampus tissues and cells were homogenized in radioimmunoprecipitation assay (RIPA) buffer (25 mM Tris·HCl at pH 7.6, 150 mM NaCl, 0.1% SDS, 1% NP-40, 1% sodium deoxycholate, and protease inhibitor (ThermoFisher, 89901)). The homogenates were then centrifuged at 12,000 rpm for 20 min at 4 °C. The protein concentration of the tissue lysate was measured with the bicinchoninic acid (BCA) assay (Thermo Fisher Scientific, 23227) after the manufacturer's protocol. Protein lysates were mixed with one-third volume of 4 × loading buffer. The supernatants were boiled and separated by sodium dodecyl sulfate polyacrylamide gel electrophoresis (SDS-PAGE). Proteins were electrophoresed and transferred to PVDF filter membranes (Merck Millipore, ISEQ00010). The membranes were blocked by incubation for 1 h with TBST (0.1% Tween 20) containing 5% non-fat milk powder (w/v), then incubated with primary antibodies. Corresponding HRP-conjugated secondary antibodies were subsequently incubated for 2 h at room temperature. Protein bands were detected by chemiluminescence using a GenoSens 2000 imaging system (Clinx Science Instruments Co., Ltd.). The primary antibodies: anti-Bmal1 (Abcam, ab93806); anti-β-actin (Proteintech, 66009-1-Ig); anti-CLOCK (Abcam, ab3517); anti-Per2 (Abcam, ab179813); anti-Cry1 (Proteintech, 13474-1-AP); anti-NeuN (Merck Millipore, ABN90); anti-PCDH19 (Abclonal, A10067); anti-PCDH19 (Abcam, ab191198); anti-Cre (Cell Signaling Technology, 15036); HRP-conjugated Affinipure Goat Anti-Mouse IgG(H + L) (Proteintech, SA00001-1); HRP-conjugated Affinipure Goat Anti-Rabbit IgG(H + L) (Proteintech, SA00001-2).

2.6. Immunofluorescence

Mice were anesthetized with isofluorane (VETEASY, RWD Life Science) and perfused transcardially with phosphate-buffered saline (PBS) followed by freshly prepared 4% polyformaldehyde. Brains were then removed, postfixed for 6 h, and gradient dehydrated with 20 and 30% sucrose in PBS. For each brain, 12 μm-thick coronal sections were cut and kept at -20℃. Permeabilize samples with 1% Triton X-100 in PBS for 15 min. Incubate samples in 10% normal goat serum in PBS for 30 min at room temperature. Sections were incubated with the following primary antibodies at 4 °C overnight: anti-Bmal1 (Abcam, ab93806), anti-NeuN (Merck Millipore, ABN90), and anti-PCDH19 (Abclonal, A10067). The sections were rinsed three times in PBS for 5 min each and then stained with corresponding fluorescence-conjugated secondary antibodies for 3 hours at room temperature. Goat Anti-Guinea pig IgG H&L (Alexa Fluor® 488) (Abcam, ab150185); Goat Anti-Rabbit IgG H&L (Cy3) (Abcam, ab6939). Finally, sections were mounted and imaged using an OLYMPUS BX53 microscope.

2.8. Stereotaxic injection of Adeno-associated virus (AAV)

Mice were anesthetized with isofluorane (VETEASY, RWD Life Science), with 4% during anesthetic induction and 1.5%~2.5% as maintenance level, and then positioned in the stereotaxic instrument. The craniotomy was drilled using a hand-held drill. The glass micropipette was used to deliver 300 nL AAV (1E + 13 VG/mL) within 60 seconds into bilateral hippocampal Dentate gyrus (DG) areas (bregma coordinates: anteroposterior − 2.40 mm; lateral-median ± 2.00 mm; dorsoventral − 2.20 mm). rAAV2/9-

hSyn-Cre-mCherry-WPRE-pA and rAAV2/9-hSyn-mCherry-WPRE-pA were purchased from BrainVTA (BrainVTA Co., Ltd., China).

2.9. High throughput sequencing (RNA sequencing analysis)

Mice were anesthetized with isofluorane (VETEASY, RWD Life Science) and perfused transcardially with phosphate-buffered saline (PBS). Put the brain tissue in pre-cooled PBS, and separate the hippocampus from brain tissue with fine tweezers. Total RNA of the hippocampus was extracted by RNeasy Mini Kit (QIAGEN, 74106). RNA samples were then further purified with magnetic oligo(dT) beads after denaturation. Purified mRNA samples were reverse transcribed into the first-strand cDNA, and a second cDNA was further synthesized. Fragmented DNA samples were blunt-ended and adenylated at the 3' ends. Adaptors were ligated to construct a library. DNA was quantified by Qubit (Invitrogen). After cBot cluster generation, DNA samples were then sequenced by an Illumina Hiseq2500 SBS from Genergy Biotechnology Co., Ltd. (Shanghai, China). Raw data were converted into Fastq format. The number of transcripts in each sample was calculated based on the number of fragments per kilobase of transcript per million fragments mapped (FPKM); Cuffnorm software was used to calculate the FPKM value for each sample, and the values were log2 transformed. DESeq2 software was used to calculate the differential gene expression between different samples. FDR (adjusted P-value) ≤ 0.05 was used to screen up-regulated or down-regulated RNAs. For the KEGG pathway analysis, the entire set of genes was used as the background list, the differential genes were used as the candidate list, and *P* was calculated. Significant genes were categorized based on gene functions. Data analysis at Genergy Biotechnology Co., Ltd. (Shanghai, China).

2.10. Statistical analysis

Differences in protein expression levels at different time points and the fluorescence intensity among three groups were analyzed by using one way ANOVA. Differences in protein expression levels and the fluorescence intensity between two groups were analyzed by using Student's *t*-test. Data of mortality rate were carried out using Fisher's exact test. The data are presented as mean ± standard error of the mean (SEM). Statistical significance was set at $p < 0.05$. The detailed statistical tests used for each analysis are stated in the figure legends. All the statistical analyses were performed with RStudio software (version 1.3.1093; https://rstudio.com/products/ rstudio/).

3. Results

3.1. Dynamic changes in Clock genes in the hippocampus after seizures

Previous studies have reported the changes in mRNA expression levels of some Clock genes [15], but the protein expression changes of these genes are still unclear. To investigate the role of circadian rhythm proteins during epileptogenesis, we examined the dynamic changes in protein levels of these proteins in mice hippocampus at the different time points after pilocarpine-induced status epilepticus (SE). The

acute phase was defined as 1 to 3 days post SE [19]. The latent phase was defined as a seizure-free period that can last weeks [20, 21]. The chronic phase was defined as mice exhibit spontaneous, recurrent seizures. Compared with the control group, Bmal1 expression was decreased at the latent phase (14 days -post-SE) and chronic phase (60 days -post-SE) (Fig. 1A and B). Clock expression was decreased at the acute (1 day -post-SE) and chronic phase, although one way ANOVA analysis is not statistically significant (Fig. 1C). There was no statistically significant change in the expression levels of Per2 and Cry1 protein (Fig. 1D - E). Because the bulk sample of hippocampus for immunoblotting detection cannot clarify which subregions of the hippocampus have decreased Bmal1 expression. The abnormal distribution of Bmal1 in the hippocampus was labeled by immunofluorescence. Compared to control, the fluorescence intensity of Bmal1 staining was reduced in the CA1 and dentate gyrus (DG) at the chronic phase (Fig. 2A - D).

3.2. Conditional knockout of Bmal1 in DG neurons increased the susceptibility to seizures

To clarify the effect of decreased Bmal1 on the epileptogenesis, AAV2/9-hSyn-Cre-mCherry or control virus were injected into the bilateral hippocampal DG area of $Bmal1^{flox/flox}$ mice (Fig. 3A). Neuron-specific knockout of Bmal1 (Bmal1 cKO) in DG significantly shortened the latency for seizures (Fig. 3B). Latency refers to the time from the pilocarpine administration (i.p.) to seizures of Racine category 4 [22]. Although there was no statistical significance, Bmal1 cKO increased the mortality rate resulted from seizures (Fig. 3C). The efficiency of Bmal1 cKO in $Bmal1^{flox/flox}$ mice was verified by immunoblotting. Compared with the control virus group, Bmal1 protein expression was significantly decreased in the cKO group (Fig. 3D - E), while Cre protein expression was significantly up-regulated in the cKO group (Fig. 3D - F).

3.3. Protocadherin 19 (PCDH19) as a potential candidate gene regulated by Bmal1

To further clarify the mechanism by which Bmal1 cKO increased the susceptibility to seizures induced by pilocarpine administration, the hippocampal tissues of Bmal1 cKO and control tissues were subjected to high-throughput sequencing. FDR (adjusted P-value) ≤ 0.05 was used to screen up-regulated or down-regulated mRNAs between the different samples. The 25 up-regulated and 19 down-regulated genes are displayed through the volcano plot and heatmap plot (Fig. 4A - C). Among these genes, PCDH19 is a gene that has been reported to be closely related to epilepsy [23]. Mutations in this gene on human chromosome X are associated with sporadic infantile epileptic encephalopathy and a female-restricted form of epilepsy [24]. PCDH19 was detected on the brain tissue slices of Bmal1 cKO (Fig. 4D). The fluorescence intensity of PCDH19 was significantly in the cKO group, compared with the control group (Fig. 4E). The level of PCDH19 in cKO was also down-regulated in the cKO group, compared with the control group (Fig. 4F - G).

3.4. Decreased expression of PCDH19 in the hippocampus of epileptic mice

Although PCDH19 mutations cause epilepsy, the expression of PCDH19 in acquired epilepsy has not been reported. Firstly, the distribution of PCDH19 in the hippocampus of TLE mice was labeled by immunofluorescence. Compared to control, the fluorescence intensity of PCDH19 staining was faint in the CA1 and DG at the chronic phase (Fig. 5A - D). The levels of PCDH19 protein were also decreased at the latent phase and the chronic phase (Fig. 5E - F).

3.5. Abnormal expression of Bmal1 and PCDH19 in hippocampal sclerosis of patients with TLE

Hippocampal sclerosis (HS) is the common histopathology in patients with drug-resistant TLE [1]. The three types of hippocampal sclerosis are classified as HS International League Against Epilepsy (ILAE) type I (severe neuronal cell loss in CA1 and CA4, 50–60% granule cell loss and granule cell dispersion (GCD)), HS ILAE type II (CA1 predominant neuronal cell loss and GCD, but usually lack severe granule cell loss) and HS ILAE type III (CA4 predominant neuronal cell loss and 35% granule cell loss) [1]. In the present study, Bmal1 and PCDH19 were detected in DG of hippocampal sclerosis tissues (HS type I and III) and the tissues without hippocampal sclerosis (no HS) by immunofluorescence. In DG, the intensity of Bmal1/NeuN and PCDH19/NeuN in the HS type I group were significantly reduced compared with no HS group (Fig. 6A - D). The intensity of Bmal1/NeuN and PCDH19/NeuN in the HS type III group was reduced compared with no HS group, although there was no statistical significance. Furthermore, the level of Bmal1 and PCDH19 in HS type I and HS type III were decreased, compared with no HS group (Fig. 6E - F).

4. Discussion

In the present study, we found that Bmal1 protein was reduced in the hippocampal DG and CA1 of mice with TLE. Neuron-specific knockout of bmal1 in DG of $Bmal1^{flox/flox}$ mice lowers the threshold of pilocarpine-induced seizures. With high-throughput sequencing and western blotting, the downstream gene PCDH19 regulated by Bmal1 was firstly identified and then detected in the hippocampus of epileptic mice. Furthermore, the expression of Bmal1 and PCDH19 were detected in HS type I, HS type III, and no HS. The levels of Bmal1 and PCDH19 protein in DG of HS type I and HS type III were decreased, compared with no HS group. These results suggest that these changes in Bmal1 and PCDH19 expression may be strongly associated with epileptogenesis and play an important role in the pathogenesis of TLE.

Circadian rhythm genes, as the important transcription factors, not only control rhythmic physiological activities such as sleep and hormone secretion, but also Clock-controlled genes (CCGs) are involved in neurodegenerative diseases, such as Alzheimer's disease and Parkinson's disease [25, 26]. In previous studies, the levels of Bmal1, CLOCK, Cry and Per mRNA have been confirmed to be decreased after drug-induced and electrically stimulated seizures in animal models [15]. The threshold of seizures induced by electrical stimulation in Bmal1 knockout (KO) mice is lower compared with the control group [16]. In the study, the knockout of clock genes is systemic, so it is unclear which organs or tissues of clock genes are knocked-out directly affect seizures. Here, the role of Bmal1 in the epileptogenesis and seizures for TLE was examined in $Bmal1^{flox/flox}$ mice with conditional deletion of Bmal1 gene in hippocampal neurons.

Our results show that Bmal1 was decreased in DG of mice and patients, and neuron-specific knockout of Bmal1in DG of Bmal1$^{flox/flox}$ mice significantly shortened the latency for seizures. This suggests that bmal may be involved in the epileptogenesis of TLE. In our study, the changes in Bmal1 expression mainly occurred in the CA1 and DG neurons. Therefore, we did not perform knockout and functional verification of Bmal1 in hippocampal astrocytes. The changed functions of astrocytes caused by Bmal1 deficiency may be involved in the pathogenesis of TLE. Astrocyte-specific Bmal1 deletion induces astrocyte activation and inflammatory gene expression in vitro and in vivo and alters circadian locomotor behavior and cognition through GABA signaling in mice [17, 18]. Astrocyte activation and gliosis are one of the common pathological symptoms of TLE [27].

At present, the molecular mechanism of Bmal1 involved in epileptogenesis has not been reported. In the present study, by using high-throughput sequencing, 25 up-regulated or 19 down-regulated mRNAs in Bmal1 cKO mice were screened (FDR $\leq$ 0.05). As one of the candidate genes, PCDH19 is a cell adhesion molecule belonging to the cadherin family. Its prominent expression is in the nervous system especially in limbic areas and cortex [24]. PCDH19 mutations result in an epileptic syndrome known as EIEE9 (OMIM # 300088). A mechanism of cellular interference has been suggested, wherein the coexistence of neurons expressing wild-type (WT) or mutant PCDH19 disrupts cell-cell interactions [28]. PCDH19 downregulation has been proved to bind and regulate $GABA_A$Rs kinetics, and increase the frequency of action potential firing [23]. PCDH19 downregulation in rat hippocampal neurons also affects the dendrite morphology [29]. Interestingly, Clock$^{flox/flox}$ mice with conditional deletion of the Clock gene in excitatory neurons also show specific spine defects and increased excitability [12]. Considering that Bmal1 and Clock are involved in transcription in the form of Bmal1:Clock complex, these indicate that the abnormal expression of Bmal1 and Clock in neurons may cause similar phenotypes and affect the epileptogenesis.

In epilepsy, DG cells formed excessive de novo excitatory connections and recurrent excitatory loops, leading to the amplification and propagation of excessive recurrent excitatory signals [30]. The granule cells' aggregate excitability has the potential to provide a therapeutic target [31]. In the present study, the expression of Bmal1 was significantly reduced in DG of patients and mice with TLE and lowered the seizure threshold via PCDH19. Therefore, DG was chosen as the target for Bmal cKO with AAV.

Clinical and animal experiments find that patients and animals with TLE show a 24-hour non-uniform distribution of seizure occurrence. These suggest that the epileptogenesis and seizures of TLE may be associated with the circadian rhythms. The two hypotheses have been proposed in seizures of TLE: (1) Rhythmic activity of molecules causes an increase in excitability periodically exceed the seizure threshold, displaying the behavioral seizures. (2) Oscillation of neuronal excitability in the suprachiasmatic nucleus (SCN) modulates the rhythmic excitability in the hippocampus via neural projections [32]. Previous studies have found that Bmal1 expression level in hippocampus still presents the circadian rhythmic oscillation in epilepsy [15]. Although the connection of nerve fibers between the suprachiasmatic nucleus and the dentate gyrus is not clear, the circadian rhythmic activity of DG has been reported in TLE [33, 34]. These suggest that the rhythmic activity of Bmal1 may cause increased excitability via PCDH19, and then periodically exceed the seizure threshold.

However, one of the disadvantages of this study is that it cannot artificially reduce the expression of Bmal1 while maintaining its periodic expression oscillation characteristics in Bmal1$^{flox/flox}$ mice with conditional deletion of the Bmal1 gene. We did not study the effect of Bmal1 KO in SCN on the epileptogenesis and seizures of TLE. Because we have not yet determined the expression changes of circadian rhythm molecules in SCN of TLE. The role of Bmal1 in the SCN of TLE will continue to be explored in the future.

In conclusion, we have disclosed a new biological function of Bmal1 in the epileptogenesis and seizures of TLE and found a downstream gene regulated by Bmal1. Our research findings may help in developing chronotherapy for mTLE, based on the chronobiology of spontaneous seizures. More detailed understandings of the role of Bmal1 and other Clock genes in the brain are required and may give novel insights into the mechanism underlying epileptogenesis and seizures of TLE.

Declarations

Ethics approval and consent to participate

This study was performed according to the Helsinki Declaration and approved by the Ethics Committee of Xi'an Jiaotong University (Ethics and Science # G-83) in full accordance with the ethical guidelines of the National Institutes of Health for the care and use of laboratory animals. We confrm that we have read the Journal's position on issues involved in ethical publication and afrm that this work is consistent with those guidelines.

Consent for publication

Not applicable.

Availability of data and materials

The datasets used and analyzed in this study are available from the corresponding authors on reasonable request.

Author contributions

Hao Wu and Hua Zhang designed the study. Hao Wu, Yong Liu, Lishuo Liu, Qiang Meng, Changwang Du, Kuo Li, Shan Dong, and Yong Zhang performed the experiments and analyzed the data. Hao Wu, Huanfa Li, and Hua Zhang wrote the paper. All authors discussed the results and revised and approved the manuscript.

Funding

This work was supported by the National Natural Science Foundation of China (NO. 81471322, 81601132) and the Institutional Foundation of The First Affiliated Hospital of Xi'an Jiaotong University

(NO. 2020ZYTS-01).

Competing interests

All authors declare no conflict of interests.

Acknowledgments

We sincerely thank the patients and their families for their participation and support in this study. This work was supported by the National Natural Science Foundation of China (NO. 81471322, 81601132) and the Institutional Foundation of The First Affiliated Hospital of Xi'an Jiaotong University (NO. 2020ZYTS-01).

References

1. Blumcke I, Thom M, Aronica E, Armstrong DD, Bartolomei F, Bernasconi A et al. International consensus classification of hippocampal sclerosis in temporal lobe epilepsy: a Task Force report from the ILAE Commission on Diagnostic Methods. Epilepsia. 2013;54(7):1315-1329.
2. Gelinas JN, Khodagholy D, Thesen T, Devinsky O, Buzsaki G. Interictal epileptiform discharges induce hippocampal-cortical coupling in temporal lobe epilepsy. Nature medicine. 2016;22(6):641-648.
3. Debski KJ, Ceglia N, Ghestem A, Ivanov AI, Brancati GE, Broer S et al. The circadian dynamics of the hippocampal transcriptome and proteome is altered in experimental temporal lobe epilepsy. Science advances. 2020;6(41).
4. Cendes F, Sakamoto AC, Spreafico R, Bingaman W, Becker AJ. Epilepsies associated with hippocampal sclerosis. Acta neuropathologica. 2014;128(1):21-37.
5. Durazzo TS, Spencer SS, Duckrow RB, Novotny EJ, Spencer DD, Zaveri HP. Temporal distributions of seizure occurrence from various epileptogenic regions. Neurology. 2008;70(15):1265-1271.
6. Spencer DC, Sun FT, Brown SN, Jobst BC, Fountain NB, Wong VS et al. Circadian and ultradian patterns of epileptiform discharges differ by seizure-onset location during long-term ambulatory intracranial monitoring. Epilepsia. 2016;57(9):1495-1502.
7. Nzwalo H, Menezes Cordeiro I, Santos AC, Peralta R, Paiva T, Bentes C. 24-hour rhythmicity of seizures in refractory focal epilepsy. Epilepsy & behavior. 2016;55:75-78.
8. Van Nieuwenhuyse B, Raedt R, Sprengers M, Dauwe I, Gadeyne S, Carrette E et al. The systemic kainic acid rat model of temporal lobe epilepsy: Long-term EEG monitoring. Brain research. 2015;1627:1-11.
9. Quigg M, Clayburn H, Straume M, Menaker M, Bertram EH, 3rd. Effects of circadian regulation and rest-activity state on spontaneous seizures in a rat model of limbic epilepsy. Epilepsia. 2000;41(5):502-509.
10. Leite Goes Gitai D, de Andrade TG, Dos Santos YDR, Attaluri S, Shetty AK. Chronobiology of limbic seizures: Potential mechanisms and prospects of chronotherapy for mesial temporal lobe epilepsy.

Neuroscience and biobehavioral reviews. 2019;98:122-134.

11. Patke A, Young MW, Axelrod S. Molecular mechanisms and physiological importance of circadian rhythms. Nature reviews Molecular cell biology. 2020;21(2):67-84.
12. Li P, Fu X, Smith NA, Ziobro J, Curiel J, Tenga MJ et al. Loss of CLOCK Results in Dysfunction of Brain Circuits Underlying Focal Epilepsy. Neuron. 2017;96(2):387-401.
13. Lipton JO, Boyle LM, Yuan ED, Hochstrasser KJ, Chifamba FF, Nathan A et al. Aberrant Proteostasis of BMAL1 Underlies Circadian Abnormalities in a Paradigmatic mTOR-opathy. Cell reports. 2017;20(4):868-880.
14. Leng Y, Musiek ES, Hu K, Cappuccio FP, Yaffe K. Association between circadian rhythms and neurodegenerative diseases. The Lancet Neurology. 2019;18(3):307-318.
15. Santos EA, Marques TE, Matos Hde C, Leite JP, Garcia-Cairasco N, Paco-Larson ML et al. Diurnal Variation Has Effect on Differential Gene Expression Analysis in the Hippocampus of the Pilocarpine-Induced Model of Mesial Temporal Lobe Epilepsy. PloS one. 2015;10(10):e0141121.
16. Gerstner JR, Smith GG, Lenz O, Perron IJ, Buono RJ, Ferraro TN. BMAL1 controls the diurnal rhythm and set point for electrical seizure threshold in mice. Frontiers in systems neuroscience. 2014;8:121.
17. Barca-Mayo O, Pons-Espinal M, Follert P, Armirotti A, Berdondini L, De Pietri Tonelli D. Astrocyte deletion of Bmal1 alters daily locomotor activity and cognitive functions via GABA signalling. Nature communications. 2017;8:14336.
18. Lananna BV, Nadarajah CJ, Izumo M, Cedeno MR, Xiong DD, Dimitry J et al. Cell-Autonomous Regulation of Astrocyte Activation by the Circadian Clock Protein BMAL1. Cell reports. 2018;25(1):1-9.
19. Kretschmann A, Danis B, Andonovic L, Abnaof K, van Rikxoort M, Siegel F et al. Different microRNA profiles in chronic epilepsy versus acute seizure mouse models. Journal of molecular neuroscience. 2015;55(2):466-479.
20. Maguire J. Epileptogenesis: More Than Just the Latent Period. Epilepsy currents. 2016;16(1):31-33.
21. Lee H, Jung S, Lee P, Jeong Y. Altered intrinsic functional connectivity in the latent period of epileptogenesis in a temporal lobe epilepsy model. Experimental neurology. 2017;296:89-98.
22. Zhang H, Gao G, Zhang Y, Sun Y, Li H, Dong S et al. Glucose Deficiency Elevates Acid-Sensing Ion Channel 2a Expression and Increases Seizure Susceptibility in Temporal Lobe Epilepsy. Scientific reports. 2017;7(1):5870.
23. Serratto GM, Pizzi E, Murru L, Mazzoleni S, Pelucchi S, Marcello E et al. The Epilepsy-Related Protein PCDH19 Regulates Tonic Inhibition, GABAAR Kinetics, and the Intrinsic Excitability of Hippocampal Neurons. Molecular neurobiology. 2020;57(12):5336-5351.
24. Gerosa L, Francolini M, Bassani S, Passafaro M. The Role of Protocadherin 19 (PCDH19) in Neurodevelopment and in the Pathophysiology of Early Infantile Epileptic Encephalopathy-9 (EIEE9). Developmental neurobiology. 2019;79(1):75-84.

25. Naismith SL, Hickie IB, Terpening Z, Rajaratnam SM, Hodges JR, Bolitho S et al. Circadian misalignment and sleep disruption in mild cognitive impairment. Journal of Alzheimer's disease : JAD. 2014;38(4):857-866.
26. Breen DP, Vuono R, Nawarathna U, Fisher K, Shneerson JM, Reddy AB et al. Sleep and circadian rhythm regulation in early Parkinson disease. JAMA neurology. 2014;71(5):589-595.
27. Pekny M, Pekna M. Astrocyte reactivity and reactive astrogliosis: costs and benefits. Physiological reviews. 2014;94(4):1077-1098.
28. Pederick DT, Richards KL, Piltz SG, Kumar R, Mincheva-Tasheva S, Mandelstam SA et al. Abnormal Cell Sorting Underlies the Unique X-Linked Inheritance of PCDH19 Epilepsy. Neuron. 2018;97(1):59-66.
29. Bassani S, Cwetsch AW, Gerosa L, Serratto GM, Folci A, Hall IF et al. The female epilepsy protein PCDH19 is a new GABAAR-binding partner that regulates GABAergic transmission as well as migration and morphological maturation of hippocampal neurons. Human molecular genetics. 2018;27(6):1027-1038.
30. Zhou QG, Nemes AD, Lee D, Ro EJ, Zhang J, Nowacki AS et al. Chemogenetic silencing of hippocampal neurons suppresses epileptic neural circuits. The Journal of clinical investigation. 2019;129(1):310-323.
31. Kahn JB, Port RG, Yue C, Takano H, Coulter DA. Circuit-based interventions in the dentate gyrus rescue epilepsy-associated cognitive dysfunction. Brain : a journal of neurology. 2019;142(9):2705-2721.
32. Cho CH. Molecular mechanism of circadian rhythmicity of seizures in temporal lobe epilepsy. Frontiers in cellular neuroscience. 2012;6:55.
33. Matzen J, Buchheim K, Holtkamp M. Circadian dentate gyrus excitability in a rat model of temporal lobe epilepsy. Experimental neurology. 2012;234(1):105-111.
34. Parekh PK, McClung CA. Circadian Mechanisms Underlying Reward-Related Neurophysiology and Synaptic Plasticity. Frontiers in psychiatry. 2016;6:187.

Table

TABLE 1.

Clincal Features of Patients with Intractable Temporal Lobe Epilepsy *

Gender	Age (years)	Epilepsy duration (years)	Seizure type	Seizure frequency	Resected tissue	Pathology	Postoperative outcome
M	20	6	SGS	1/month	LTB;H	Gliosis	II
M	43	20	SGS	2/month	LTB;H	Gliosis	I
M	20	2	SGS	1/month	RTB;H	Gliosis	
F	13	3	SGS	15/month	RTB;H	Gliosis	II
M	15	5	SGS	2/month	RT-OB	Gliosis	I
M	32	9	CPS	2/month	LTB;H	Gliosis	
M	21	19	SGS	60/month	RTB;H	Gliosis	
M	22	0.17	CPS	4/month	RTB;H	Gliosis	
F	21	10	CPS	1/month	LTB;H	Gliosis	
F	26	7	CPS	45/month	RTB;H	Gliosis	
F	22	4	SGS	160/month	RTB;H	Gliosis	I
M	18	5	CPS	1/month	RTB;H	Gliosis	
M	35	20	SGS	3/month	LTB;H	Gliosis	II
F	13	0.33	SGS	1-3/day	RTB;H	Gliosis	I
F	26	11	SGS	1/month	RTB;H	Gliosis	I
M	39	14	SGS	3-4/month	LTB;H	Gliosis	II
F	30	7	SGS	2-3/month	LTB;H	Gliosis	I
M	23	7	SGS	15/month	LTB;H	Gliosis	I

***SGS**, secondarily generalized seizures; **CPS**, complex partial seizures; **LTB**, left temporal lobe; **RTB**, right temporal lobe; **H**, hippocampus; **FCD**, focal cortical dysplasia; **Postoperative outcome**, Engel's class.

Figures

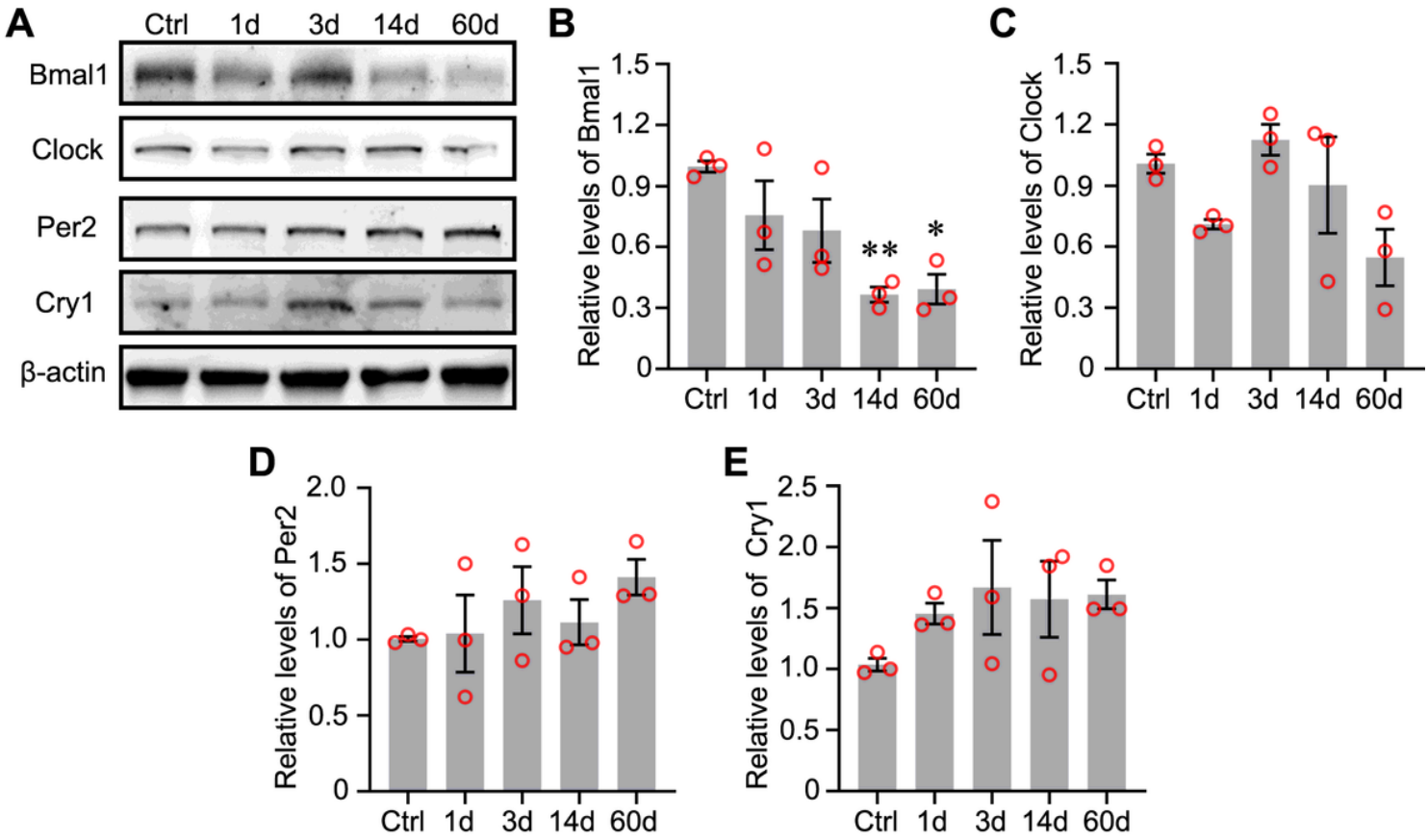

Figure 1

Expression of Circadian rhythm proteins in mouse hippocampus following pilocarpine-induced status epilepticus (SE). (A) Changes in protein levels of Circadian rhythm proteins at different time points following pilocarpine-induced SE. (B - E) Comparison of Bmal1 blots density between control mice and epileptic mice at each time point after SE (n=3 per group). Bmal1 expression was significantly decreased at 14 d (0.366 ± 0.038) and 60 d (0.393 ± 0.073), compared with Ctrl (0.995 ± 0.027). There is no significant difference in the Clock, Per2 and Cry1 expression levels between control group and epileptic groups at different time points. The data are expressed as mean ± SEM and analyzed with one-way ANOVA. *$p < 0.05$, **$p < 0.01$.

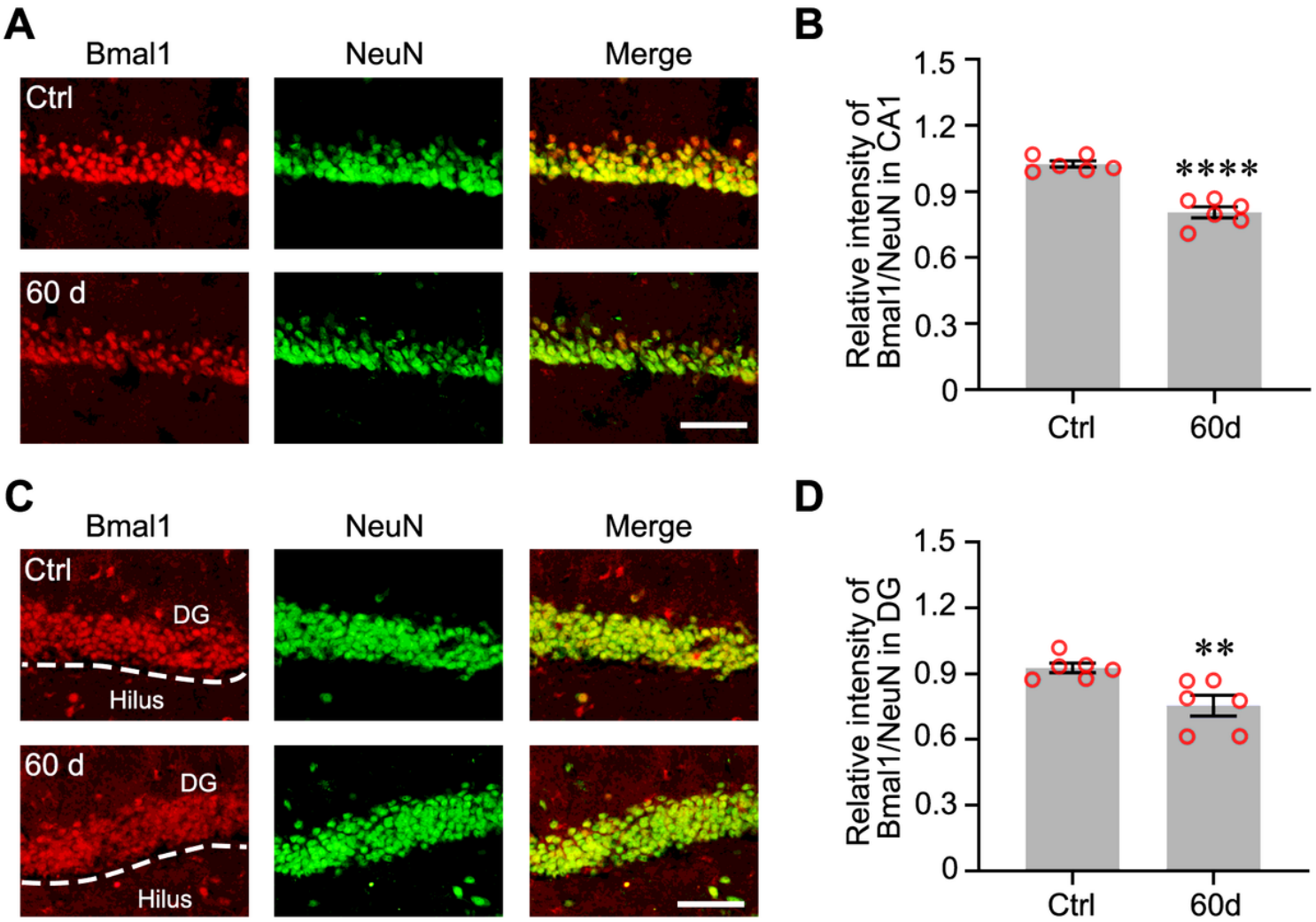

Figure 2

Immunofluorescence detection of Bmal1 expression in the hippocampal CA1 and DG of epileptic mice. (A) Detection of the endogenous Bmal1 protein (red) in CA1 by immunofluorescent labeling. Neurons were labeled by the neuronal marker, NeuN (green). Scale bar, 100 μm. (B) Analysis of fluorescence intensity was performed using ImageJ. Differences in the relative fluorescence intensity (Bmal1 vs. NeuN) were analyzed with the Students t-test (Control: 1.025 ± 0.015, 60 d: 0.805 ± 0.025, n=3, $p < 0.0001$). (C) Detection of Bmal1 protein (red) and NeuN (green) in DG by immunofluorescent labeling. Scale bar, 100 μm. (D) Analysis of fluorescence intensity was performed using ImageJ. Differences in the relative fluorescence intensity (Bmal1 vs. NeuN) were analyzed with the Students t-test (Control: 0.926 ± 0.022, 60 d: 0.755 ± 0.047, n=3, $p=0.008$). The data are expressed as mean ± SEM and analyzed with unpaired Student's t-test. $^{**}p < 0.01$, $^{***}p < 0.001$.

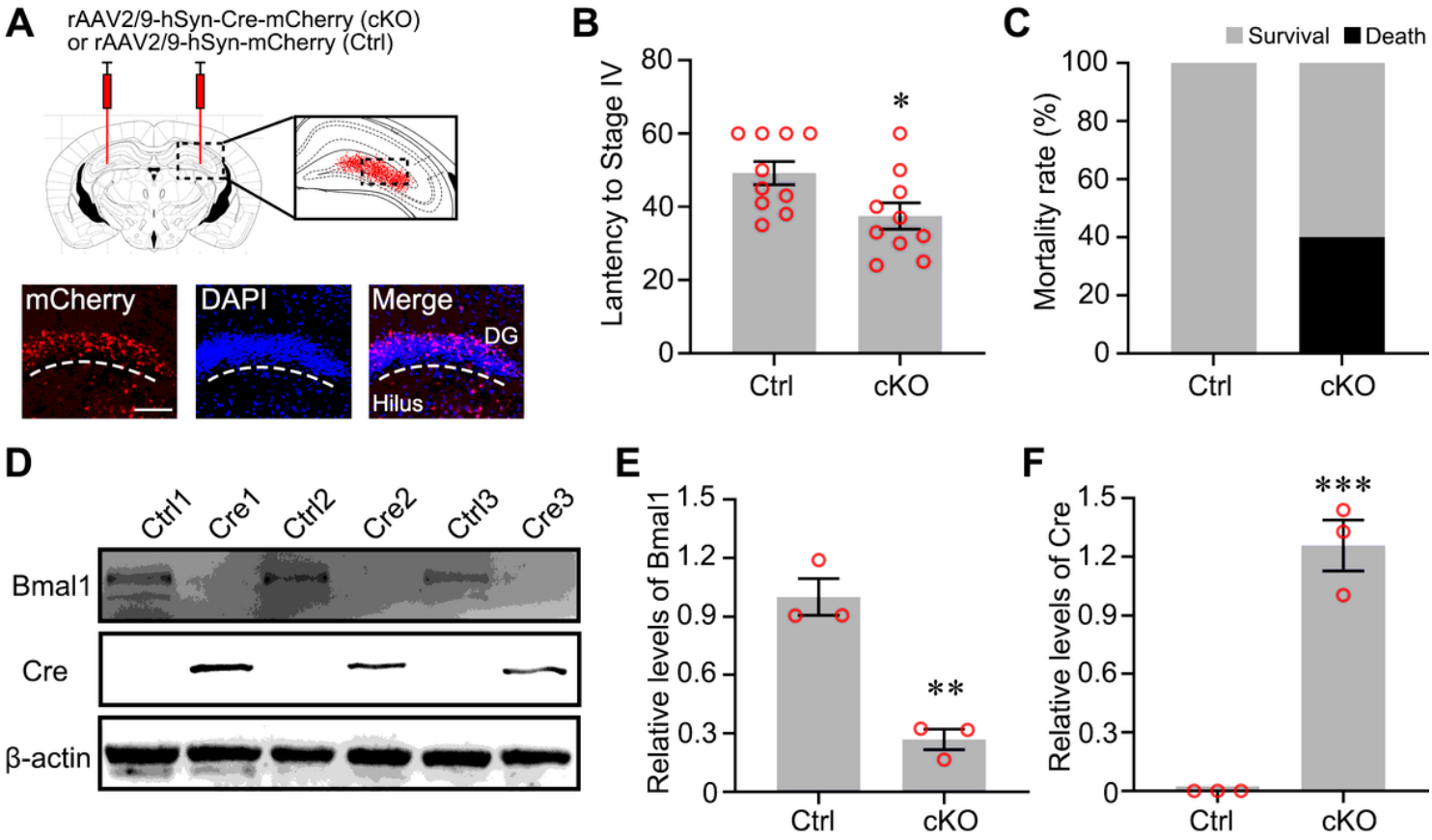

Figure 3

Conditional knockout (cKO) of Bmal1 in DG neurons increased the susceptibility to seizures. (A) Schematic diagram of AAV injection and the expression of mCherry encoded by an AAV carrying mCherry in DG neurons. Scale bar, 100 μm. (B) Seizure behavior assessment in control group (n=10) and cKO group (n=10) after pilocarpine administration. Data of latency (control: 49.20 ± 3.193; cKO: 37.50 ± 3.583, p=0.025) are presented as mean ± SEM and analyzed using unpaired Student's t-test. (C) Data of mortality rate in control group and cKO group (n=10, p=0.094) were carried out using Fisher's exact test. (D) The efficiency of Bmal1 cKO in Bmal1flox/flox mice verified by immunoblotting. Bmal1 expression was significantly decreased at cKO group, compared with Ctrl group. Differences in the levels of Bmal1 are presented as mean ± SEM and analyzed using unpaired Student's t-test (control: 1.000 ± 0.095, 0.270 ± 0.052, n=3, p=0.003). (E) Cre expression was significantly increased at cKO group, compared with Ctrl group. Differences in the levels of Cre are presented as mean ± SEM and analyzed using unpaired Student's t-test (control: 0, cKO: 1.257 ± 0.131, n=3, p=0.0007). *p < 0.05, **p < 0.01, ***p < 0.001.

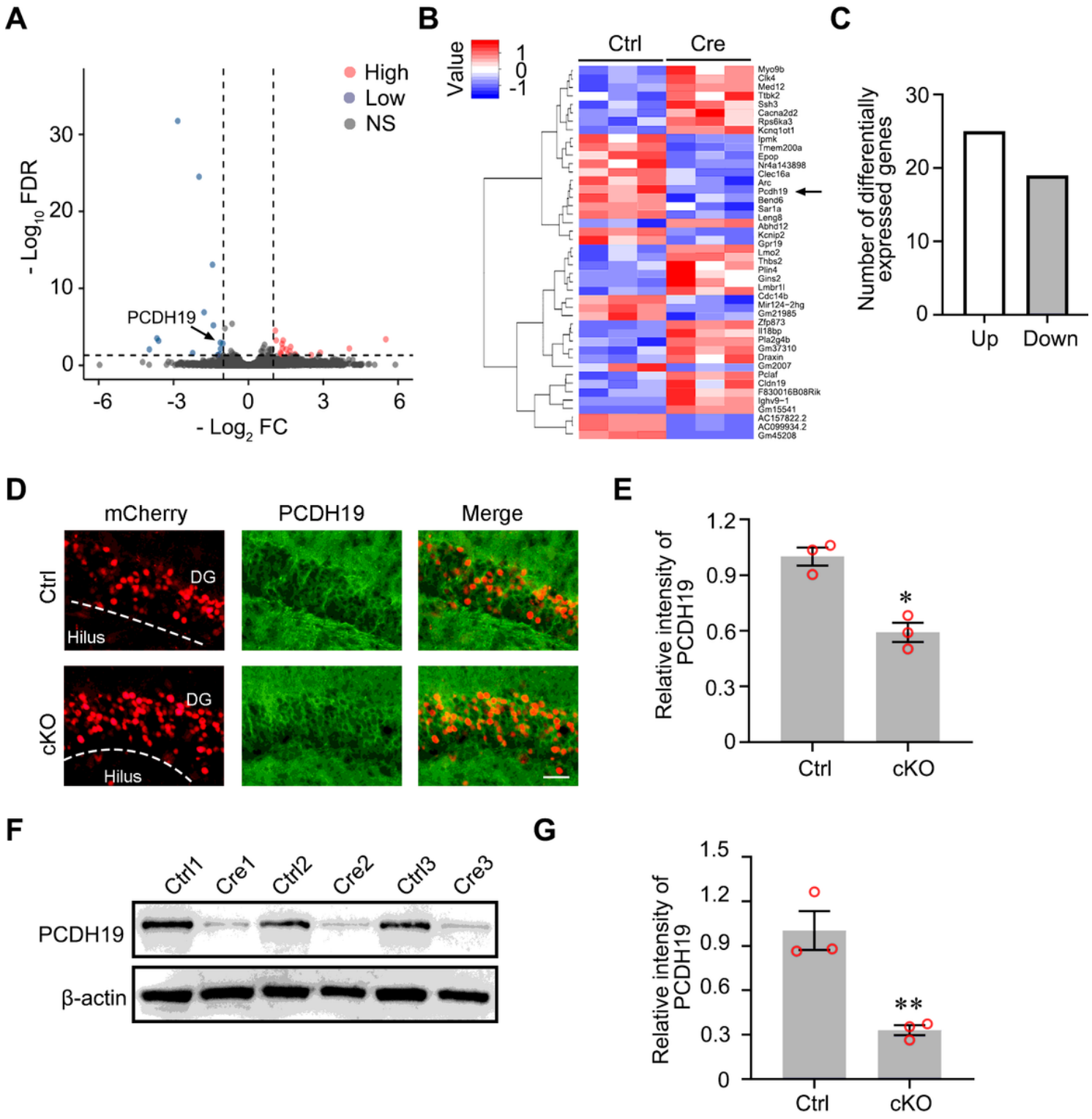

Figure 4

PCDH19 as a potential candidate gene regulated by Bmal1. (A) The volcano plot of differentially expressed genes between control group and cKO group (FDR < 0.05). (B) Heat map of significantly up- or down-regulated genes between control group and cKO group. Each group contained three batches of individual samples. (C) The number of the significantly differentially expressed genes between control group and cKO group (fold change > 2, FDR < 0.05). (D - E) Immunofluorescence detection of mCherry

and PCDH19 expression in DG of mice. Scale bar, 50 μm. Analysis of fluorescence intensity was performed using ImageJ. Differences in the intensity between control group and cKO group were analyzed with the Students t-test (Control: 1.000 ± 0.049, cKO: 0.592 ± 0.052, n=3, p=0.007). (F - G) PCDH19 expression was significantly increased at cKO group, compared with Ctrl group. Differences in the levels of PCDH19 are presented as mean ± SEM and analyzed using unpaired Student's t-test (control: 1.003 ± 0.131, cKO: 0.330 ± 0.033, n=3, p=0.008). The data are expressed as mean ± SEM and analyzed with unpaired Student's t-test. *p < 0.05, **p < 0.01.

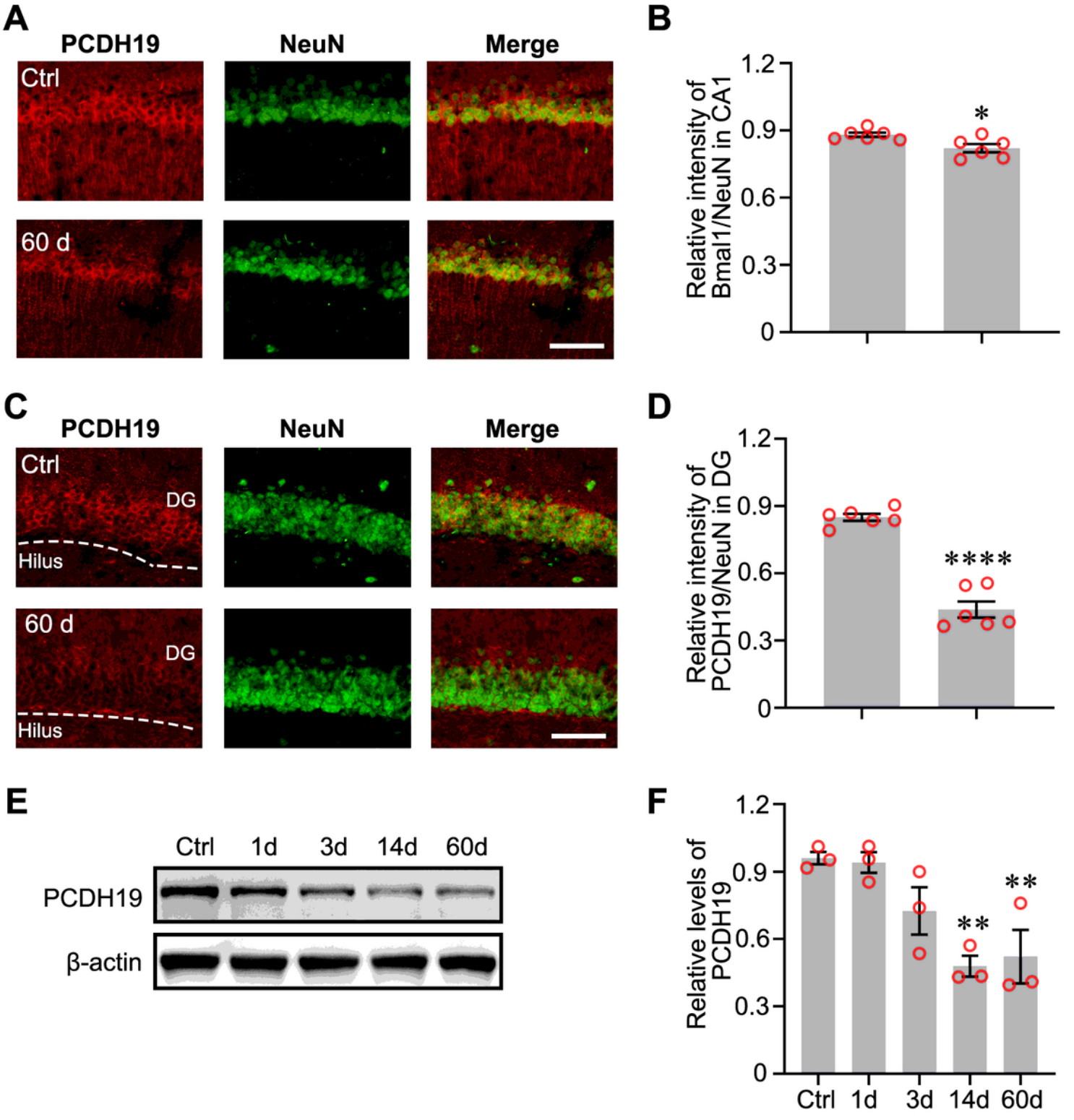

Figure 5

PCDH19 expression in the hippocampal CA1 and DG of epileptic mice. (A) Detection of the endogenous PCDH19 protein (red) in CA1 by immunofluorescent labeling. Neurons were labeled by the neuronal marker, NeuN (green). Scale bar, 100 μm. (B) Analysis of fluorescence intensity was performed using ImageJ. Differences in the relative fluorescence intensity (PCDH19 vs. NeuN) were analyzed with the Students t-test (Control: 0.987 ± 0.006, 60 d: 0.947 ± 0.012, n=3, p=0.015). (C) Detection of PCDH19 protein (red) and NeuN (green) in DG by immunofluorescent labeling. Scale bar, 100 μm. (D) Analysis of fluorescence intensity was performed using ImageJ. Differences in the relative fluorescence intensity (PCDH19 vs. NeuN) were analyzed with the Students t-test (Control: 0.967 ± 0.010, 60 d: 0.693 ± 0.024, n=3, $p < 0.0001$). The data are expressed as mean ± SEM and analyzed with unpaired Student's t-test. **$p < 0.01$, *$p < 0.05$, ****$p < 0.0001$. (E) The levels of PCDH19 protein at different time points following pilocarpine-induced SE. (F) Comparison of PCDH19 blots density between control mice and epileptic mice at each time point after SE (n=3 per group). Bmal1 expression was significantly decreased at 14 d (0.480 ± 0.046) and 60 d (0.522 ± 0.119), compared with Ctrl (0.960 ± 0.028). The data are expressed as mean ± SEM and analyzed with one-way ANOVA, **$p < 0.01$.

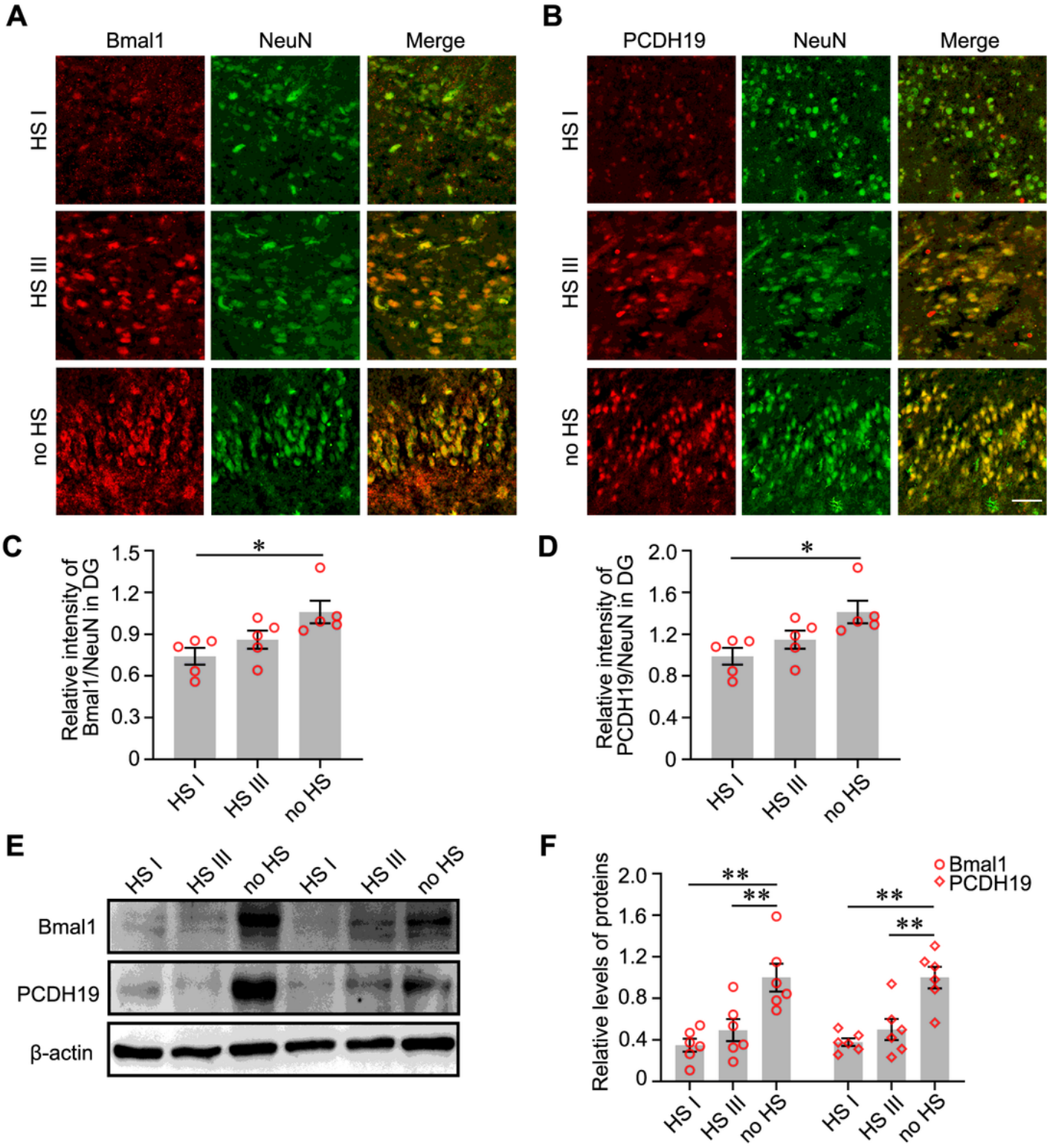

Figure 6

Bmal1 and PCDH19 expression in the hippocampal DG of patients with TLE. (A -B) Detection of the endogenous Bmal1 and PCDH19 protein (red) in DG of HS type I, HS type III and no HS by immunofluorescent labeling. Neurons were labeled by the neuronal marker, NeuN (green). Scale bar, 100 μm. (C) Analysis of fluorescence intensity was performed using ImageJ. Differences in the relative fluorescence intensity (Bmal1 vs. NeuN) among the three groups were analyzed with one-way ANOVA,

compared with no HS (HS I: 0.741 ± 0.060, HS III: 0.860 ± 0.651, no HS:1.059 ± 0.081, n=5). (D) Differences in the relative fluorescence intensity (PCDH19 vs. NeuN) among the three groups were analyzed with one-way ANOVA, compared with no HS (HS I: 0.739 ± 0.079, HS III: 1.044 ± 0.093, no HS:1.160 ± 0.157, n=5). (E) The levels of Bmal1 and PCDH19 protein in hippocampus of HS type I, HS type III and no HS by immunoblotting. (F) Differences in the levels of Bmal1 among the three groups were analyzed with one-way ANOVA, compared with no HS (For Bmal1, HS I: 0.350 ± 0.062, HS III: 0.494 ± 0.106, no HS:1.000 ± 0.135, n=6; For PCDH19, HS I: 0.379 ± 0.037, HS III: 0.501 ± 0.102, no HS:1.000 ± 0.105, n=6;). *p < 0.05, **p < 0.01.